Iranaian J. Numerical Analysis and Optimization
Vol. 3, No. 1, (2013), 55-72

Finite volume method for one dimensional biot poroelasticity system in multilayered domains

M. Namjoo and H. Atighi Lorestani

Abstract

R. Ewing, O. Liev, R. Lazarov and A. Naumovich in [1] proposed a finite volume discretization for one dimensional Biot poroelasticity system in multilayer domains. Their discretization and exact solution are invalid. We derive valid discretization and exact solution. Finally, our numerical solution is compared with known exact solution in discrete L_2 norm.

Keywords: Biot poroelasticity system; Interface problem; Finite volume discretization.

1 Introduction

The presence of a moving fluid in a porous medium affects its mechanical response. At the same time, the change in the mechanical state of the porous skeleton influences the behavior of the fluid inside the pores. These two coupled deformation-diffusion phenomena lie at the heart of the theory of poroelasticity. More precisely, the two key phenomena can be summarized as follows:

1. fluid-to-solid coupling: occurs when a change in the fluid pressure or the fluid mass induces a deformation of the porous skeleton.
2. solid-to-fluid coupling: occurs when modifications in the stress of the porous skeleton induce change in the fluid pressure or the fluid mass.

In accordance with these two phenomena, the fluid-filled porous medium acts in a time-dependent manner. Indeed, suppose that the porous medium is compressed. This will result in an increment of the fluid pressure inside the pores and consequent fluid flow. The time dependence of the fluid pressure will induce a time dependence of the poroelastic stresses, which in turn will respond

M. Namjoo
Department of Mathematics, Vali-e-Asr University of Rafsanjan, Rafsanjan, Iran. e-mail: namjoo@vru.ac.ir

H. Atighi Lorestani
Department of Mathematics, Vali-e-Asr University of Rafsanjan, Rafsanjan, Iran. e-mail: hatighi@gmail.com

back to the fluid pressure field. The earliest theories, which is related to Terzaghi, accounted for the fluid-to-solid coupling only. In this case, the problem is mathematically much easier. This kind of theory can model successfully some of the poroelastic processes in the case of highly compressible fluids such as air. However, when one deals with slightly compressible or incompressible fluids, the solid-to-fluid coupling cannot be neglected since the changes in stress field can influence significantly the pore pressure. Maurice Biot was the first who, by means of phenomenological approach, developed a detailed mathematical theory of poroelasticity which successfully incorporated both basic phenomena mentioned above. In this paper, assumption of only vertical subsidence is invoked and this leads to the one dimensional model of poroelasticity. We consider a finite volume discretization for one dimensional Biot poroelasticity system in multilayer domains. For stability reasons, staggered grids are used. The discretization takes into account discontinuity of the coefficients across the interfaces between layers with different physical properties.

2 Biot model in one dimension

In one dimension, the domain of consideration Ω is an interval $(0, L)$ where the boundary Γ is $\{0, L\}$. The Biot model, which describes poroelastic process in Ω can be written as a system of partial differential equations for the unknown fluid pressure $p(x, t)$ and displacement of the porous medium $u(x, t)$ consisting of the equilibrium equation and the diffusion equation

$$\begin{cases} -\dfrac{\partial}{\partial x}((\lambda + 2\mu)\dfrac{\partial u}{\partial x}) + \dfrac{\partial p}{\partial x} = 0, \quad x \in (0, L), \quad t \in (0, T], \\ \dfrac{\partial}{\partial t}(\phi\beta p + \dfrac{\partial u}{\partial x}) - \dfrac{\partial}{\partial x}(\dfrac{\kappa}{\eta}\dfrac{\partial p}{\partial x}) = q(x, t), \quad x \in (0, L), \quad t \in (0, T], \end{cases}$$

where λ (dilation moduli) and μ (shear moduli) are Lame coefficients of the porous medium. Here ϕ, β, κ, η and $q(x, t)$ are porosity of porous medium, compressibility of the fluid, permeability of the porous medium, viscosity of the fluid and source term, respectively. We define stress tensor and fluid velocity, respectively by the following relationships

$$S = (\lambda + 2\mu)\frac{\partial u}{\partial x}, \quad V = -\frac{\kappa}{\eta}\frac{\partial p}{\partial x}.$$

In classical formulation, the one-dimensional Biot model describes, fluid flow and skeleton deformation caused by the constant vertical load applied on the top of column of soil, which is bounded with rigid and impermeable bottom and lateral walls, and a top wall which is free to drain. The following boundary

and initial conditions supplement this model

$$p = 0, \quad (\lambda + 2\mu)\frac{\partial u}{\partial x} = -s_0, \quad at \quad x = 0.$$

This means that the upper boundary is free to drain and a load with the value s_0 is applied to it. Also

$$u = 0, \quad \frac{\partial p}{\partial x} = 0, \quad at \quad x = L,$$

corresponds to a rigid and impermeable lower boundary. The initial condition

$$\phi\beta p + \frac{\partial u}{\partial x} = 0, \quad at \quad t = 0,$$

means that the variation in water content is zero at the beginning of the process. Now, consider the case when the porous medium is not homogeneous but has a layered structure, each layer being characterized by different porosity, permeability and Lame coefficients. For the simplicity of presentation, let us restrict ourselves to the case of only two layers. In the case of the considered two-layered medium, coefficients of the governing equations are discontinuous across the interface ξ

$$\lambda(x) = \begin{cases} \lambda_1 & x \leq \xi, \\ \lambda_2 & x > \xi, \end{cases} \qquad \mu(x) = \begin{cases} \mu_1 & x \leq \xi, \\ \mu_2 & x > \xi, \end{cases}$$

$$\kappa(x) = \begin{cases} \kappa_1 & x \leq \xi, \\ \kappa_2 & x > \xi, \end{cases} \qquad \phi = \begin{cases} \phi_1 & x \leq \xi, \\ \phi_2 & x > \xi. \end{cases}$$

Assuming a perfect contact, the interface conditions look as follows

$$[u] = 0, \quad [p] = 0, \tag{1}$$

which express continuity of the displacement and of the fluid pressure across the interface. Also

$$[S] = 0, \quad [V] = 0, \tag{2}$$

which means continuity of the stress of the porous skeleton and continuity of the fluid flux, respectively. In the formulae (1) and (2), we have

$$[q] = q\mid_{x=\xi+0} - q\mid_{x=\xi-0},$$

where q is a symbol for quantities u, p, S and V. As it is shown in [3], the set of interface conditions (1) and (2) can also be derived directly from the Biot equations if they are written for a general inhomogeneous medium. Now, the following dimensionless dependent and independent functions are introduced

$$x := \frac{x}{L}, \quad \xi := \frac{\xi}{L}, \quad t := \frac{(\lambda_0 + 2\mu_0)\kappa_0 t}{\eta_0 L^2}, \quad p := \frac{p}{s_0}, \quad u := \frac{(\lambda_0 + 2\mu_0)u}{s_0 L},$$

$$\nu := \frac{\lambda + 2\mu}{\lambda_0 + 2\mu_0}, \quad \kappa := \frac{\frac{\kappa}{\eta}}{\frac{\kappa_0}{\eta_0}}, \quad a := \phi\beta(\lambda_0 + 2\mu_0), \quad f(x,t) := \frac{L^2\eta_0}{s_0\kappa_0} q(x,t).$$

Then, the governing equations together with the boundary, initial and interface conditions can be transformed to dimensionless form

$$\begin{aligned}
&-\frac{\partial}{\partial x}(\nu\frac{\partial u}{\partial x}) + \frac{\partial p}{\partial x} = 0, \quad x \in (0,1), \quad t \in (0,T], \\
&\frac{\partial}{\partial t}(ap + \frac{\partial u}{\partial x}) - \frac{\partial}{\partial x}(\kappa\frac{\partial p}{\partial x}) = f(x,t), \quad x \in (0,1), \quad t \in (0,T], \\
&\nu\frac{\partial u}{\partial x} = -1, \quad p = 0, \quad at \quad x = 0, \quad t \in [0,T], \\
&u = 0, \quad \kappa\frac{\partial p}{\partial x} = 0, \quad at \quad x = 1, \quad t \in [0,T], \\
&ap + \frac{\partial u}{\partial x} = 0, \quad at \quad t = 0, \quad x \in (0,1), \\
&[u] = 0, \quad [\nu\frac{\partial u}{\partial x}] = 0, \quad [p] = 0, \quad [\kappa\frac{\partial p}{\partial x}] = 0, \quad at \quad x = \xi, \quad t \in [0,T].
\end{aligned} \tag{3}$$

Further, the possible discontinuities of the dimensionless coefficients at $x = \xi$ are distinguished

$$\nu(x) = \begin{cases} \nu_1 & x \le \xi, \\ \nu_2 & x > \xi, \end{cases} \qquad \kappa(x) = \begin{cases} \kappa_1 & x \le \xi, \\ \kappa_2 & x > \xi, \end{cases}$$

$$a(x) = \begin{cases} a_1 & x \le \xi, \\ a_2 & x > \xi. \end{cases}$$

For the convenience of the theoretical analysis, the problem (3) is transformed into a problem with homogeneous boundary conditions, by the following substitution

$$u(x,t) := u(x,t) - \frac{1}{\nu}x + \frac{1}{\nu}.$$

According to this substitution, problem (3) is reformulated as follows:

$$
\begin{aligned}
&-\frac{\partial}{\partial x}(\nu\frac{\partial u}{\partial x})+\frac{\partial p}{\partial x}=0, \quad x\in(0,1), \quad t\in(0,T],\\
&\frac{\partial}{\partial t}(ap+\frac{\partial u}{\partial x})-\frac{\partial}{\partial x}(\kappa\frac{\partial p}{\partial x})=f(x,t), \quad x\in(0,1), \quad t\in(0,T],\\
&\nu\frac{\partial u}{\partial x}=0, \quad p=0, \quad at \quad x=0, \quad t\in[0,T],\\
&u=0, \quad \kappa\frac{\partial p}{\partial x}=0, \quad at \quad x=1, \quad t\in[0,T],\\
&ap+\frac{\partial u}{\partial x}=\frac{1}{\nu}, \quad at \quad t=0, \quad x\in(0,1),\\
&[u]=0, \quad [\nu\frac{\partial u}{\partial x}]=0, \quad [p]=0, \quad [\kappa\frac{\partial p}{\partial x}]=0, \quad at \quad x=\xi, \quad t\in[0,T].
\end{aligned}
\tag{4}
$$

Due to the complexity of the Biot system, analytical solutions in closed form are available only in very special cases. Certainly, the situation gets complicated in the case of inhomogeneous porous media. The choice of the numerical method for the discretization of the poroelasticity system is not obvious. The finite element method currently dominates in solving poroelasticity system, especially when dealing with complex domains (see [4] for further details). Although finite element methods can be applied to the interface problems, however, they usually work on grids which resolve the interfaces. Hence this fact leads to that imposes certain restriction on the method. Moreover, even when the grids resolve the interfaces, standard finite element methods do not provide good approximation for the flux variables. On the other hand, there is variety of successful finite difference and finite volume approaches, where the interfaces are allowed to cross the grid cells (see [5]).

2.1 Grids and notations

For the interval $(0,1)$ and $N>1$, we define stepsize h in the following form

$$h:=\frac{2}{2N-1}.$$

To overcome stability difficulties, which often arise when the discretization of the Biot model is done on the collocate grids, the use of staggered grids was proposed in [2], [7]. Two different spatial grids, $\bar{\omega}_p$ to discretize the pressure equation and $\bar{\omega}_u$ to discretize the displacement equation, are employed

$$
\begin{aligned}
&\bar{\omega}_p=\{x_i: \quad x_i=ih, \ i=0,1,...,N-1\},\\
&\bar{\omega}_u=\{x_{i-0.5}: \quad x_{i-0.5}=x_i-0.5h, \ i=1,2,...,N\}.
\end{aligned}
$$

Further, the grids ω_p and ω_u are also used

$$\omega_p = \{x_i \in \bar{\omega}_p, \quad i = 1, 2, ..., N-1\},$$
$$\omega_u = \{x_{i-0.5} \in \bar{\omega}_u, \quad i = 1, 2, ..., N-1\}.$$

A grid in time with a stepsize τ is also defined

$$\omega_T = \{t_n : \quad t_n = n\tau, \quad n = 1, 2, ..., M\}.$$

These grids as designed to represent the values of the pressure p at the grid points $x_i \in \bar{\omega}_p$ and the values of the displacement u at the midpoints $x_{i-0.5} \in \bar{\omega}_u$ of the subintervals (x_{i-1}, x_i). According to these grids, position of the interface ξ could be represented in the form

$$\xi = x_{i_{int}-0.5} + \theta h,$$

where $0 < i_{int} < N$ is an integer and $0 \leq \theta < 1$. Now, the following notations for discrete functions, defined on $\bar{\omega}_u \times \omega_T$ and $\bar{\omega}_p \times \omega_T$, respectively, are introduced

$$u := u^n := u_i^n := u(x_{i-0.5}, t_n),$$
$$p := p^n := p_i^n := p(x_i, t_n),$$
$$p^\sigma := \sigma p^{n+1} + (1-\sigma)p^n,$$
$$p^\wedge := p^{n+1}.$$

Moreover we use some notations for the first order forward and backward finite differences on a uniform mesh in the following form

$$p_x := p_{x,i} = \frac{p(x_{i+1}, t) - p(x_i, t)}{h},$$
$$p_{\bar{x}} := p_{\bar{x},i} = \frac{p(x_i, t) - p(x_{i-1}, t)}{h}.$$

In a similar way we define

$$u_x := u_{x,i} = \frac{u(x_{i+0.5}, t) - u(x_{i-0.5}, t)}{h},$$
$$u_{\bar{x}} := u_{\bar{x},i} = \frac{u(x_{i-0.5}, t) - u(x_{i-1.5}, t)}{h}.$$

Finally, the finite differences in time are defined

$$u_t := u_t^n := u_t(x_{i-0.5}, t_n) = \frac{u_i^{n+1} - u_i^n}{\tau}, \quad x_{i-0.5} \in \omega_u,$$
$$p_t := p_t^n := p_t(x_i, t_n) = \frac{p_i^{n+1} - p_i^n}{\tau}, \quad x_i \in \omega_p.$$

2.2 Finite volume discretization

In order to approximate the differential problem (4) by finite volume method. Firstly the Biot equations are rewritten in the following way

$$\begin{aligned} -\frac{\partial S}{\partial x} + \frac{\partial p}{\partial x} &= 0, \quad x \in (0,1), \quad t \in (0,T], \\ \frac{\partial}{\partial t}(ap + \frac{\partial u}{\partial x}) + \frac{\partial V}{\partial x} &= f(x,t), \quad x \in (0,1), \quad t \in (0,T]. \end{aligned} \tag{5}$$

Now, the first equation in (5) is integrated over the interval (x_{i-1}, x_i)

$$-\int_{x_{i-1}}^{x_i} \frac{\partial S}{\partial x} dx + \int_{x_{i-1}}^{x_i} \frac{\partial p}{\partial x} dx = 0, \tag{6}$$

and the second equation over the interval $(x_{i-0.5}, x_{i+0.5})$

$$\int_{x_{i-0.5}}^{x_{i+0.5}} \frac{\partial}{\partial t}(ap + \frac{\partial u}{\partial x}) dx + \int_{x_{i-0.5}}^{x_{i+0.5}} \frac{\partial V}{\partial x} dx = \int_{x_{i-0.5}}^{x_{i+0.5}} f(x,t) dx. \tag{7}$$

Hence, in accordance with the interface conditions (1) and (2), some integrals from (6) and (7) can be rewritten as

$$\begin{aligned} &\int_{x_{i-1}}^{x_i} \frac{\partial S}{\partial x} dx = S(x_i) - S(x_{i-1}), \quad \int_{x_{i-0.5}}^{x_{i+0.5}} \frac{\partial V}{\partial x} dx = V(x_{i+0.5}) - V(x_{i-0.5}), \\ &\int_{x_{i-1}}^{x_i} \frac{\partial p}{\partial x} dx = p(x_i) - p(x_{i-1}), \quad \int_{x_{i-0.5}}^{x_{i+0.5}} \frac{\partial u}{\partial x} dx = u(x_{i+0.5}) - u(x_{i-0.5}). \end{aligned} \tag{8}$$

Using the rectangular quadratic formula, we can write

$$\int_{x_{i-0.5}}^{x_{i+0.5}} \frac{\partial}{\partial t}(ap) dx \approx \frac{\partial p}{\partial t}(x_i) \int_{x_{i-0.5}}^{x_{i+0.5}} a(x) dx \approx a_i \frac{p_i^{n+1} - p_i^n}{\tau},$$

where

$$a_i = \int_{x_{i-0.5}}^{x_{i+0.5}} a(x) dx. \tag{9}$$

In order to approximate the fluxes $S(x)$ and $V(x)$ in (8) in the grid points, with integrating the equation

$$\frac{S(x)}{\nu} = \frac{\partial u}{\partial x},$$

over the interval $(x_{i-0.5}, x_{i+0.5})$ and the equation

$$\frac{V(x)}{\kappa} = -\frac{\partial p}{\partial x},$$

over the interval (x_{i-1}, x_i) we will have the following integral equations

$$\int_{x_{i-0.5}}^{x_{i+0.5}} \frac{S(x)}{\nu} dx = \int_{x_{i-0.5}}^{x_{i+0.5}} \frac{\partial u}{\partial x} dx, \quad \int_{x_{i-1}}^{x_i} \frac{V(x)}{\kappa} dx = -\int_{x_{i-1}}^{x_i} \frac{\partial p}{\partial x} dx.$$

Then, by applying approximate formulae for integrals, we can transform these equations into the following form

$$S(x_i) \int_{x_{i-0.5}}^{x_{i+0.5}} \frac{dx}{\nu(x)} dx \approx u_{i+0.5} - u_{i-0.5}, \quad V(x_{i-0.5}) \int_{x_{i-1}}^{x_i} \frac{dx}{\kappa(x)} dx \approx -(p_i - p_{i-1}).$$

From these two formulae, approximate expressions for fluxes can be found

$$S(x_i) \approx S_i = \nu_i \frac{u_{i+0.5} - u_{i-0.5}}{h}, \quad V(x_{i-0.5}) \approx V_i = -\kappa_i \frac{p_i - p_{i-1}}{h},$$

where

$$\nu_i = (\frac{1}{h} \int_{x_{i-0.5}}^{x_{i+0.5}} \frac{dx}{\nu(x)})^{-1}, \quad \kappa_i = (\frac{1}{h} \int_{x_{i-1}}^{x_i} \frac{dx}{\kappa(x)})^{-1}. \tag{10}$$

After the substitution of approximate expressions for all the integrals into equations (6) and (7), weighted discretization in time with the weight parameter σ is applied. This procedure produces a finite difference scheme, which is a discrete analogue of the problem (4). The obtained finite difference scheme is theoretically investigated and detailed convergence analysis is presented in [6]. Using non-index notations, this scheme for the discrete approximate solution $u = u_i^n$ at point $(x_{i-0.5}, t_n) \in \omega_u \times \omega_T$ and $p = p_i^n$ at grid point $(x_i, t_n) \in \omega_p \times \omega_T$ can be written as in the following form

$$-\tfrac{\nu}{h} u_x^{\wedge} + p_{\bar{x}}^{\wedge} = 0, \quad x = x_{0.5} \ (i = 1), \quad t \in \omega_T, \quad \nu(x) = \begin{cases} \nu_1 & x \le \xi, \\ \nu_2 & x > \xi. \end{cases}$$

$$-\nu_1 (u_{\bar{x}}^{\wedge})_x + p_{\bar{x}}^{\wedge} = 0, \quad x_i \le \xi, \ (i = 2, 3, ..., N-1), \quad t \in \omega_T,$$

$$-\tfrac{\nu_2}{h} u_x^{\wedge} + \tfrac{\nu_1}{h} u_{\bar{x}}^{\wedge} + p_{\bar{x}}^{\wedge} = 0, \quad x_{i-1} \le \xi, \quad x_i > \xi, \ (i = 2, 3, ..., N-1), \quad t \in \omega_T,$$

$$-\nu_2 (u_{\bar{x}}^{\wedge})_x + p_{\bar{x}}^{\wedge} = 0, \quad x_{i-1} > \xi, \ (i = 2, 3, ..., N-1), \quad t \in \omega_T,$$

$$(ap + u_x)_t - \kappa_1 (p_{\bar{x}}^{\sigma})_x = f^{\sigma}, \quad x_{i-0.5} \le \xi, \ (i = 1, 2, ..., N-2), \quad t \in \omega_T, \tag{11}$$

$$(ap + u_x)_t - \tfrac{\kappa_2}{h} p_x^{\sigma} + \tfrac{\kappa_1}{h} p_{\bar{x}}^{\sigma} = f^{\sigma}, \quad x_{i-0.5} \le \xi, \ x_{i+0.5} > \xi, \ (i = 1, 2, ..., N-2), \quad t \in \omega_T,$$

$$(ap + u_x)_t - \kappa_2 (p_{\bar{x}}^{\sigma})_x = f^{\sigma}, \quad x_{i-0.5} > \xi, \ (i = 1, 2, ..., N-2), \quad t \in \omega_T,$$

$$(ap + u_x)_t + \tfrac{\kappa}{h} p_{\bar{x}}^{\sigma} = f^{\sigma}, \quad x = x_{N-1}, \ (i = N-1), \quad t \in \omega_T, \quad \kappa(x) =$$

$$\begin{cases} \kappa_1 & x_{N-1.5} \leq \xi, \\ \kappa_2 & x_{N-1.5} > \xi. \end{cases}$$

$$p_0 = 0, \quad u_N = 0, \quad t \in \omega_T,$$

$$ap + u_x = \tfrac{1}{\nu}, \quad x = x_i \in \bar{\omega}_p, \ (i = 1, 2, ..., N-1), \quad t = 0,$$

where coefficients a, κ and ν are calculated according to the formula (9), (10) and the right hand side f is defined as

$$f_i(t) = \frac{1}{h} \int_{x_{i-0.5}}^{x_{i+0.5}} f(x,t)dx.$$

3 Numerical results

In this section, results of the numerical experiment are presented. Convergence of all unknowns of the system, i.e., u and p produced by the scheme (11) with respect to the exact solution of the continuous problem are shown. The numerical solution is compared to the known exact solution in discrete L_2 norm, which is calculated according to the following form

$$\|\varepsilon_w\|_{L_2} = h \sum_{x_i \in \omega_w} |w_{ext}(x_i, t_{n+1}) - w_{app}(x_i, t_{n+1})|^2,$$

where w_{ext} and w_{app} stand for the exact and numerical solutions, respectively and $w = \{u, p\}$. In the following experiment, weight parameter is $\sigma = 0.5$.

Example 3.1 Suppose the following values of the parameters are used:

$$\begin{aligned} &\nu_1 = 1, \quad \nu_2 = \frac{\tan(\frac{1}{12})\tan(\frac{10\pi}{3})}{8\pi}, \\ &\kappa_1 = 1, \quad \kappa_2 = \frac{1}{8\pi \tan(\frac{1}{12})\tan(\frac{10\pi}{3})}, \\ &a_1 = 0, \quad a_2 = 0, \quad f(x,t) = 0. \end{aligned}$$

The position of the interface is at $\xi = \frac{1}{6}$. There is no exact solution of problem (4). Now, consider the following initial condition

$$(a-1)p + \nu \frac{\partial u}{\partial x} = 0 \quad at \quad t = 0.$$

If we substitute the above condition in problem (4), the exact solution is as the following forms

$$p(x,t) = \begin{cases} \cos(\frac{10\pi}{3})\sin(\frac{x}{2})\exp(-0.25t) & x \le \xi, \\ \\ \sin(\frac{1}{12})\cos(4\pi(1-x))\exp(-0.25t) & x > \xi, \end{cases}$$

$$u(x,t) = \begin{cases} -2\cos(\frac{10\pi}{3})\cos(\frac{x}{2})\exp(-0.25t) & x \le \xi, \\ \\ -2\frac{\cos(\frac{1}{12})}{\tan(\frac{10\pi}{3})}\sin(4\pi(1-x))\exp(-0.25t) & x > \xi. \end{cases}$$

Note that the mesh size h is decreased in a way, preserving a constant value for the parameter θ in the expression $\xi = x_{i-0.5} + \theta h$. The convergence results are given for times $t = 0.1$ and $t = 1$. All numerical results are shown in Tables 1 and 2. In Figures 3.1(a-e) and 3.2(f-j), we have the convergence

Table 1: Convergence in discrete L_2 norm at the time $t = 0.1$.

$h = \tau$	$\|\varepsilon_u\|$	$\|\varepsilon_p\|$
$\frac{1}{10}$	0.010978550724151	$2.584356430578406 \times 10^{-5}$
$\frac{1}{40}$	$4.299657739862227 \times 10^{-7}$	$1.565023743780048 \times 10^{-6}$
$\frac{1}{160}$	$5.255105309209073 \times 10^{-9}$	$4.642021997862129 \times 10^{-7}$
$\frac{1}{640}$	$5.263842780036844 \times 10^{-10}$	$2.411707866280830 \times 10^{-7}$
$\frac{1}{2560}$	$3.408942895693747 \times 10^{-11}$	$6.152003882582387 \times 10^{-8}$

Table 2: Convergence in discrete L_2 norm at the time $t = 1$.

$h = \tau$	$\|\varepsilon_u\|$	$\|\varepsilon_p\|$
$\frac{1}{10}$	$6.010657532287119 \times 10^{-5}$	$2.069371443954429 \times 10^{-5}$
$\frac{1}{40}$	$2.741582817269723 \times 10^{-7}$	$9.979031969906696 \times 10^{-7}$
$\frac{1}{160}$	$3.350803084864384 \times 10^{-9}$	$2.959883906284094 \times 10^{-7}$
$\frac{1}{640}$	$3.356374342242523 \times 10^{-10}$	$1.537772829030507 \times 10^{-7}$
$\frac{1}{2560}$	$2.173637957624389 \times 10^{-11}$	$3.922690864486794 \times 10^{-8}$

of displacement for given stepsizes h=0.1, 1/40, 1/160, 1/640 and 1/2560 at t=0.1 and t=1, respectively. Also, Figures 3.3(k-o) and 3.4(p-t) are prepared for representation of convergence of pressure for given stepsizes h=0.1, 1/40, 1/160, 1/640 and 1/2560 at t=0.1 and t=1, respectively. In all of these figures, exact and approximate solutions are represented by continuous lines and broken lines, respectively.

Figure 3.1(a)

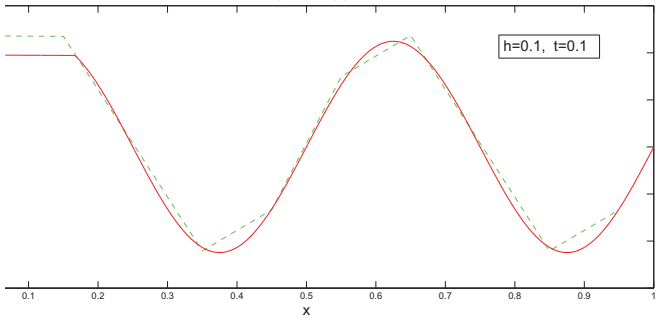

Figure 3.1(b)

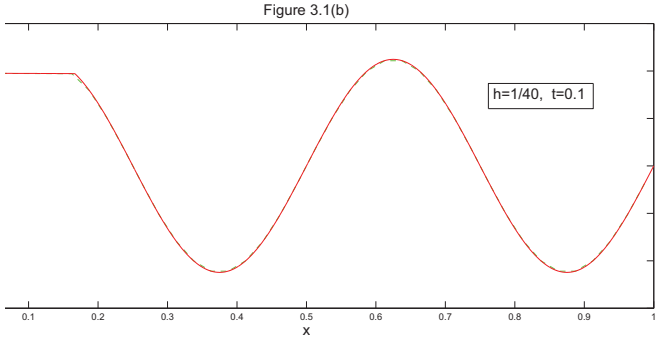

Figure 3.1(c)

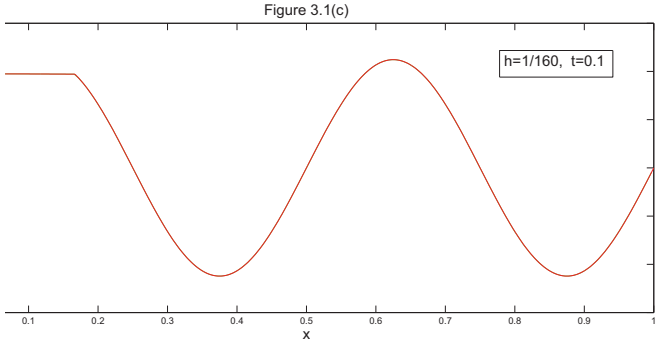

Figure 3.1(d)

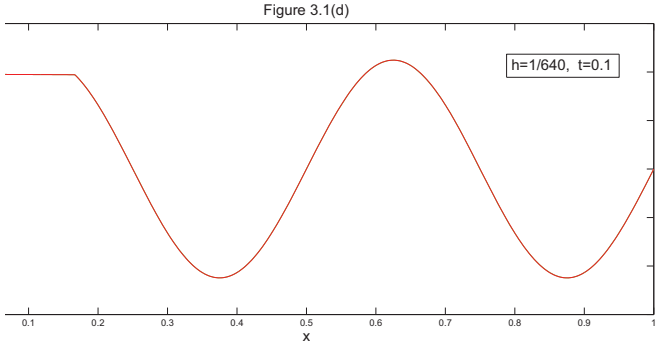

Figure 3.1(e)

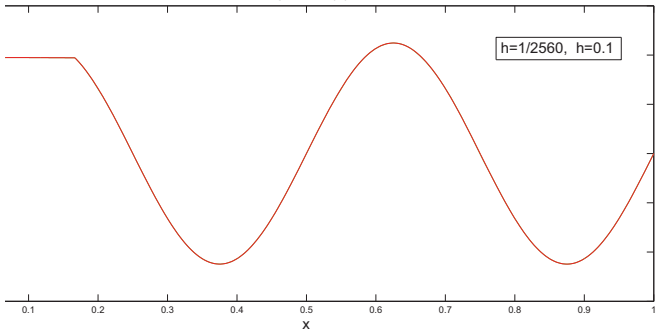

Figure 3.2(f)

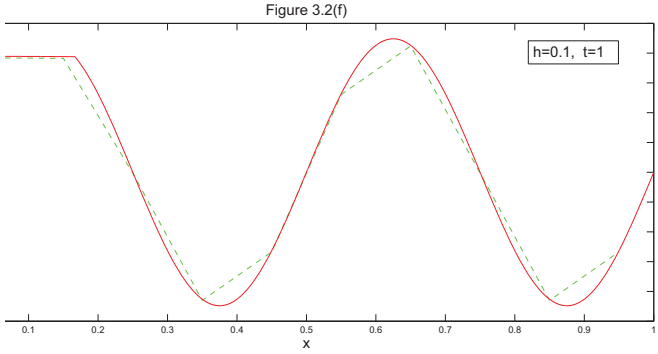

Figure 3.2(g)

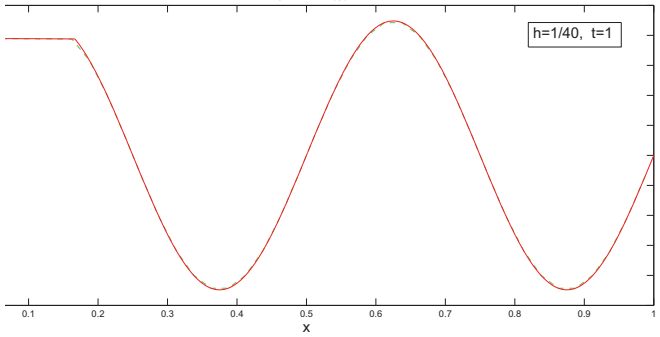

Figure 3.2(h)

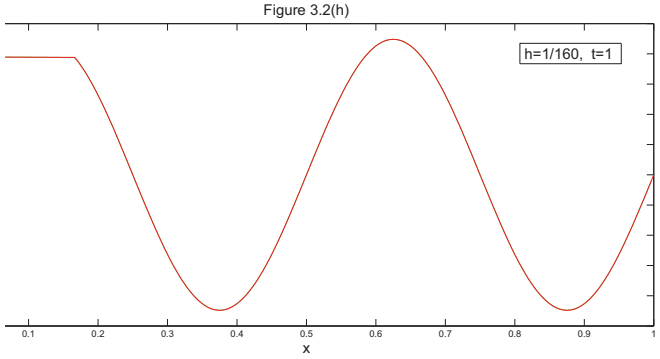

Figure 3.2(i)

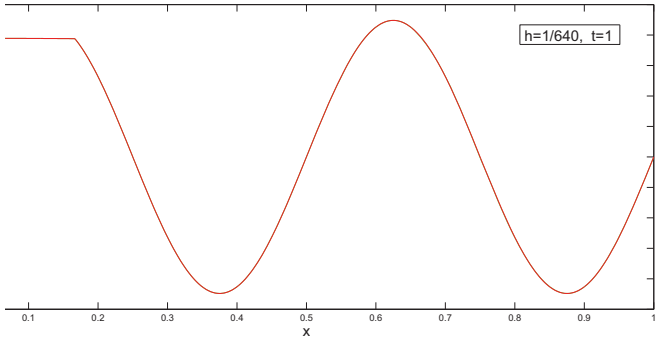

Figure 3.2(j)

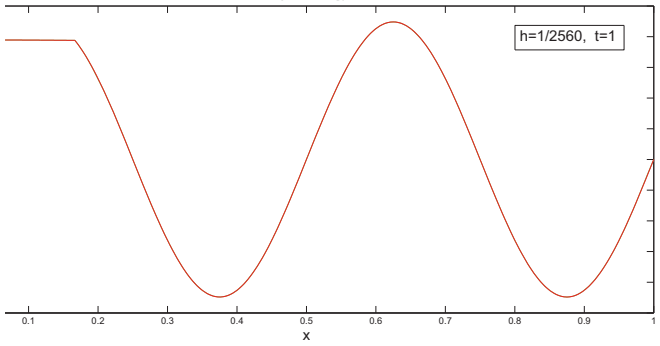

Figure 3.3(k)

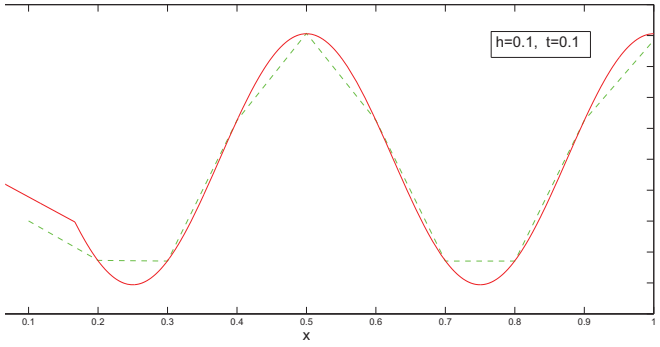

Figure 3.3(l)

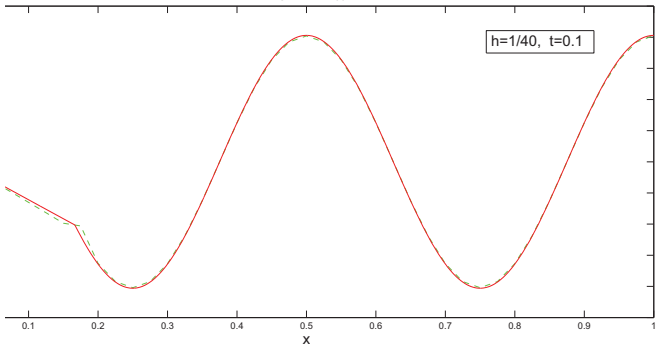

Figure 3.3(m)

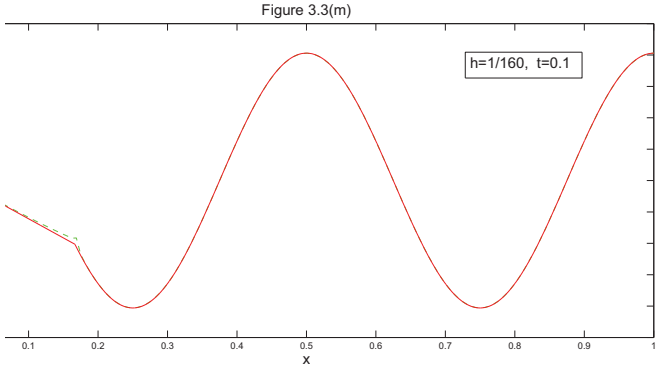

Figure 3.3(n)

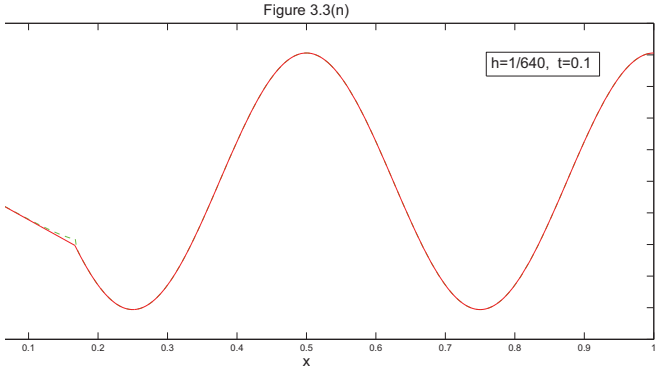

Figure 3.3(o)

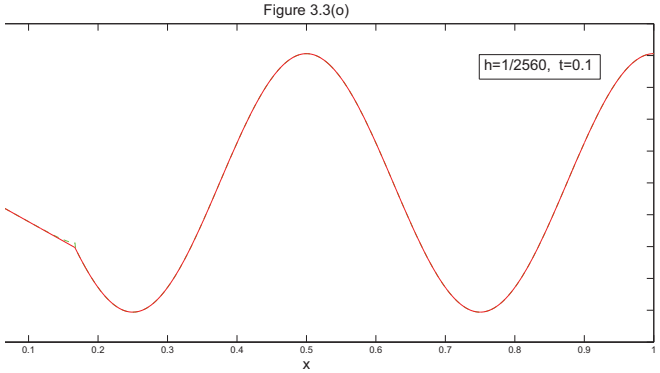

Figure 3.4(p)

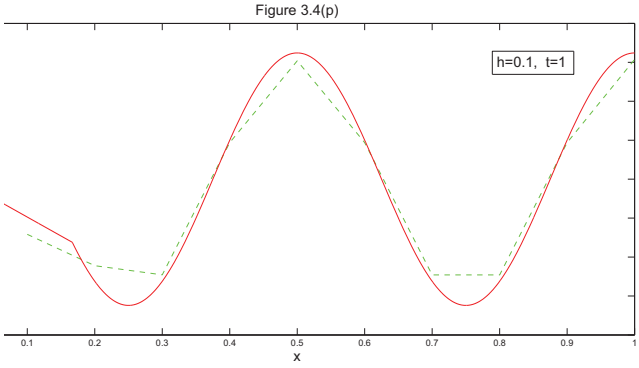

Figure 3.4(q)

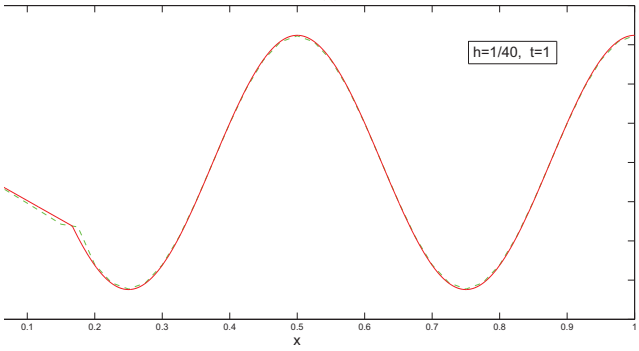

Figure 3.4(r)

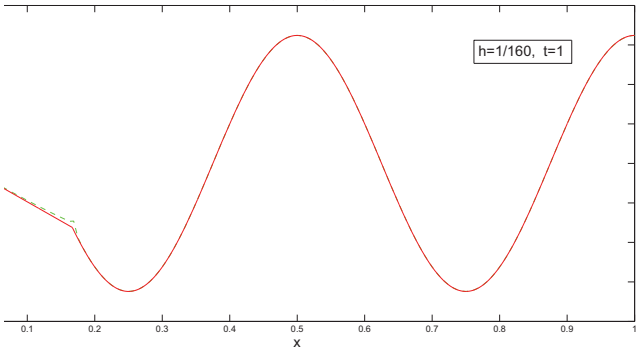

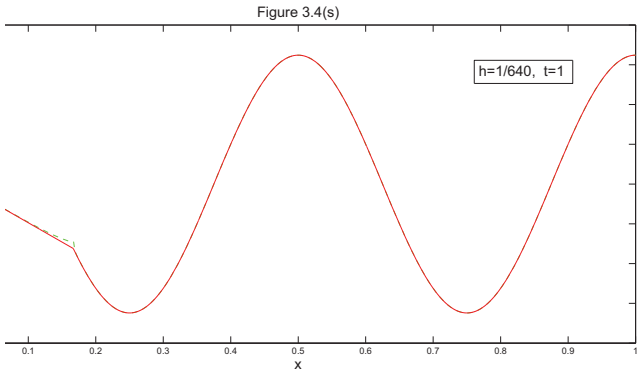

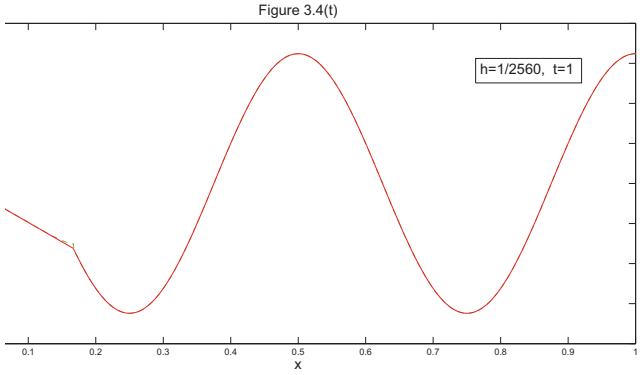

4 Conclusion

In this paper, we derived a finite volume discretization for the Biot system with continuous coefficients. In example 3.1, numerical solution was compared to the known exact solution in descrete L_2 norm. In Tables 1 and 2 and derived figures, when the stepsize h becames smaller, we derived better results. In fact, our numerical experiments confirmed the theoretical considerations.

References

1. Ewing, R., Liev, O., Lazarov, R. and A. Naumovich, *On convergence of certain finite volume difference discretizations for 1D poroelasticity interface problems*, Wiley InterScience, DOI 10. 1002/ num. 20184, (2006).
2. Gaspar, F. J., Lisbona, F. J. and Vabishchevich, P. N., *A finite difference analysis of Biot' s consolidation model*, Departamento de Matematica Aplicada, University of Zaragoza, Zaragoza, Spain., Applied numerical mathematics **4**, (2003), 487-506.
3. Gurevich, B. and Schoenberg, M., *Interface conditions for Biot' s equations of poroelasticity*, J. Acoust. Soc. Am., **105** (5), (1999), 2585-2589.
4. Korsawe, J. and Starke, G., *A least - squares mixed finite element method for Biot's consolidation problem in porous media* , SIAM Journal on numerical analysis, **43** (1), (2005), 318 - 339.
5. Liev, O., *Finite volume discretizations for elliptic problems with discontinuous coefficients*, Habilitation, University of Kaiserslautern, (2002).
6. Naumovich, A., *Efficient numerical methods for the Biot poroelasticity system in multilayered domains*, Vom fachbereich mathematik, Der universitat kaiserslautern, Zur verleihung des akademischen grades, (2007).
7. Versteeg, H. K. and Malalaskera, W., *An introduction to computational fluid dynamics*: The finite volume method, Longman scientific and technical, (1995).